Structure of cereulide, a cyclic dodecadepsipeptide toxin from *Bacillus cereus* and studies on NMR characteristics of its alkali metal complexes including a conformational structure of the K^+ complex

Sathorn Suwan,[a] Minoru Isobe,*[,a] Ikuko Ohtani,[a] Norio Agata,[b] Masashi Mori[b] and Michio Ohta[c]

[a] *Lab. of Organic Chemistry, School of Agricultural Sciences, Nagoya University, Chikusa, Nagoya 464-01, Japan*
[b] *Nagoya City Public Health Research Institute, 1–11 Hagiyamacho, Mizuhoku, Nagoya 467, Japan*
[c] *Department of Bacteriology, School of Medicine, Nagoya University, 65 Tsurumaicho, Showa-ku, Nagoya 466, Japan*

The structure and stereochemistry of cereulide **1** or **1a**, an emetic toxin produced by *Bacillus cereus*, have been determined through spectral analysis and chemical methods. It is a 36-membered cyclic depsipeptide with the sequence of *cyclo*(D-*O*-Leu-D-Ala-L-*O*-Val-L-Val)$_3$. The outstanding property of cereulide is a Rb^+- and K^+-ion-selective ionophore, the same as in valinomycin **2**. Cereulide forms a 1:1 complex with alkali metal ions. Owing to its structural similarity to valinomycin **2** and our well established conformational knowledge about compound **2**, the NMR data of cereulide–alkali metal complexes in chloroform gave us a partial view of the conformational structure in solution and a calculated modelling of the complex with K^+ is proposed. The main chain shows a hexagonal cyclinder-like framework which is similar to the known bracelet-like structure of the valinomycin–K^+ complex. All amide carbonyls arrange along the cylindrical side-wall planes so that they can form β-turn hydrogen bonds with NH protons. Every alpha carbon is located at a corner in both the top and the bottom planes, enabling alpha protons of oxy acids to turn inwards towards the cavity and those of the amino acids turn outwards. The K^+ is centrally situated in the cavity of the host cereulide by the ion–dipole interactions with three carbonyl oxygens of L-Val in the top plane and the three carbonyls of D-Ala in the bottom plane. The experimental coupling constant and NOE data of the K^+ complex had conformity with the calculated dihedral angle and distance measured from the proposed conformational structure. Partial views of the conformations of cereulide complexed with Li^+ and Na^+ are analysed as follows: The frameworks of the Li^+ complex main chain lose their compactness, becoming more linearly extended, which results in a bigger cavity diameter, have fewer hydrogen bonds, and all the residual side-chains can freely rotate whereas the conformation(s) of the Na^+ complex takes the intermediate conformation(s) between those of the highly stable (the K^+ and Rb^+) and that of the less stable (the Li^+) complexes.

An emetic toxin has been recognized as the cause of *Bacillus cereus* emetic-syndrome food poisoning since 1976.[1] Limited information was available on this toxin molecule mainly because the valid *in vitro* bioassay method had not been well established. The emetic activity of a crude sample was retained after exposure to high temperatures such as 126 °C for 90 min or to digestion with trypsin or pepsin.[2] The toxin was assumed to be a small-molecular-mass compound of M_r less than 5000.[2–4] Recently, we obtained the chemically pure toxin from a culture broth of *B. cereus* by 7 purification steps including precipitation, partition, silica gel chromatography and reversed-phase HPLC.[5] The toxin activity was monitored by a bioassay observing formation of vacuoles in HEp-2 cells according to Hughes *et al.*[6] The final preparation eluted as a single peak at t_R 8.3 min on an ODS-5 column (250 × 10 mm) using 95% MeOH–water containing 0.1% trifluoroacetic acid (TFA) as mobile phase at a flow rate of 4.7 cm^3 min^{-1}. The toxin was a white powder and was named cereulide. The minimum dose required to form vacuoles in HEp-2 cells was ~5 ng cm^{-3}. During the course of structural elucidation, cereulide **1** showed its intrinsic ability to bind with some metals such as potassium and sodium ions. Accordingly, we thought that cereulide may have properties as an ionophore. The structure of compound **1** was found to resemble that of valinomycin **2**, a well known antibiotic having selective binding properties to Rb^+ and K^+ and which biologically behaves as a K^+-carrier ionophore. The present study describes details of the structural elucidation of cereulide and proposes a higher structure of the cereulide–K^+ complex in chloroform including comparative views of the conformations of the complexes with other metal ions based on FAB-MS and proton NMR data of cereulide complexes with alkali metal ions, plus those of valinomycin **2** complexes.

Results and discussion

Assignment of planar structure and stereogenic centres

Fig. 1 shows a ^1H NMR spectrum (600 MHz) of cereulide **1** in $(CD_3)_2SO$ ([$^2H_6$]DMSO). It shows 2 sets of doublet NH signal (δ 8.0–8.4), 4 alpha protons (δ 4.2–5.1) and 7 sets of doublet methyl signals (δ 0.7–1.4). The ^{13}C NMR (150 MHz) spectrum of compound **1** showed 4 sets of carbonyl signals (δ_C 168.9, 169.4, 170.5 and 171.4). The double quantum filtered (DQF)-COSY and homonuclear Hartmann–Hahn (HOHAHA) spectra indicated 4 partial structures. The first one was assigned as alanine (Ala) because one doublet NH signal (δ 8.35) correlated with a quartet-doublet α-proton (δ 4.37) and doublet methyl signal (δ 1.35). The second component was recognizable as valine (Val) from the correlations among the doublet NH signal (δ 8.03), doublet-doublet α-proton (δ 4.31), multiplet β-proton (δ 2.18) and two doublet methyl signals (δ 0.90 and 0.89). The third one had no NH signal, and there were only the correlations among doublet α-proton (δ 4.83), multiplet β-proton (δ 2.10) and two doublet methyl signals (δ 0.85 and 0.80). Therefore, 2-hydroxy-3-methylbutyric acid (*O*-Val) was assigned as one of the partial structures. Similarly, the fourth

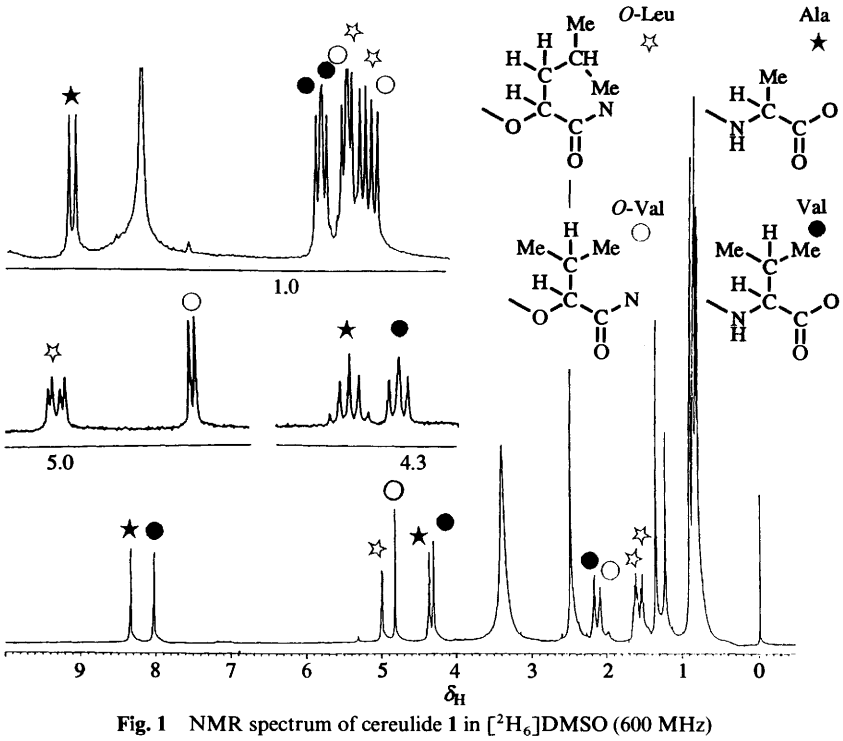

Fig. 1 NMR spectrum of cereulide **1** in [$^2H_6$]DMSO (600 MHz)

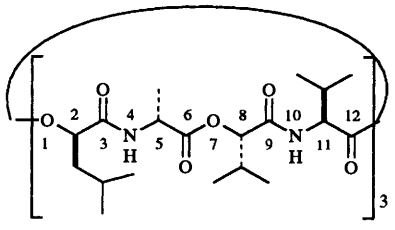

D-*O*-Leu D-Ala L-*O*-Val L-Val

Cereulide **1**

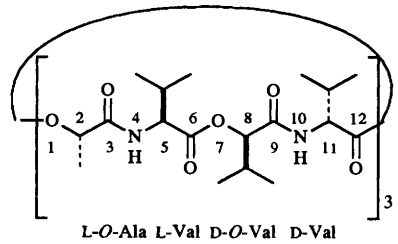

L-*O*-Ala L-Val D-*O*-Val D-Val

Valinomycin **2**

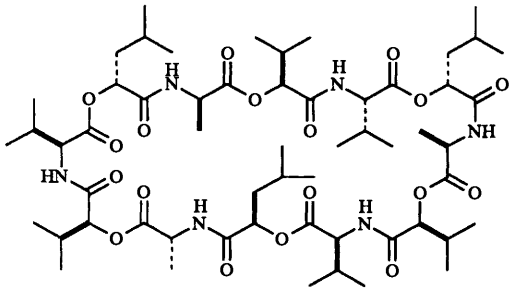

Cereulide **1a**

component was assigned as 2-hydroxy-4-methylvaleric acid (*O*-Leu), its doublet-doublet α-proton (δ 5.00) being in the same spin system with two multiplet β-protons (δ 1.53 and 1.64), multiplet γ-proton (δ 1.60) and two doublet methyl signals (δ 0.84 and 0.82). The 2D heteronuclear multiple-bond coherence (HMBC) data indicating component connectivity are specially shown in bold in Table 1. Thus, coupling signals appeared between the carbonyl carbon of *O*-Leu (C-3, δ_C 169.4) and NH of Ala (4-H, δ 8.35). The carbonyl carbon of Ala (C-6, δ_C 171.4) coupled with α-H of *O*-Val (8-H, δ 4.83). These connectivities suggested the sequence of *O*-Leu-Ala-*O*-Val. Similarly, the carbonyl carbon of *O*-Val (C-9) was observed to correlate with NH of Val (10-H) and the carbonyl carbon of Val (C-12) had correlation with α-H of *O*-Leu (2-H). These indicated another sequential connectivity of *O*-Val-Val-*O*-Leu. Alternating peptide and ester bonds are also consistent with the fact that alpha protons of amino acids appeared at higher chemical shifts than those of oxy acids. Only these four kinds of components were indicated from the NMR data. Consequently, the structure of cereulide was temporarily assigned as a 12-membered cyclic tetra-depsipeptide with the sequence *cyclo*-(*O*-Leu-Ala-*O*-Val-Val).

FAB-MS analysis, however, did not give the corresponding peak for the cyclic tetra-depsipeptide structure ($C_{19}H_{32}N_2O_6$ M_r = 384). The positive FAB-MS of cereulide gave two peaks at *m/z* 1191 and 1171 instead and the negative FAB-MS gave a major peak at *m/z* 1151. These data suggested that the relative molecular mass was 1152, three times the major that of the temporary structure; thus, *m/z* 1191, 1171 and 1151 matched with $(M + K)^+$, $(M + H_3O)^+$ and $(M - H)^-$, respectively. The high-resolution positive FAB-MS afforded *m/z* 1191.643 (as potassium complex); calc. for $(C_{19}H_{32}N_2O_6)_3K^+$: *m/z* 1191.642. Therefore, the molecular formula became $C_{57}H_{96}N_6O_{18}$; thus, the molecular structure of cereulide **1** is a 36-membered cyclic depsipeptide with the sequence *cyclo*-(*O*-Leu-Ala-*O*-Val-Val)$_3$.

Since the structure of compound **1** was composed of alternating amino and oxy acid residues, it enabled us to determine the stereogenic centres in two steps of alkali and subsequent acid hydrolyses. Thus, cereulide **1**, which was treated with 1.2 mol dm^{-3} KOH at 50 °C for 2 h, gave two dipeptide components, *viz*. *O*-Leu-Ala **3** and *O*-Val-Val **4**

Table 1 ^1H and ^{13}C NMR data of cereulide **1** in [$^2H_6$]DMSO

Residue	Assignment	^1H δ, mult.[a] [J (Hz)]	^{13}C[b] δ	HMBC[c]	ROESY
D-*O*-Leu	**2**	**5.00**, dd (9.8, 3.5)	71.7	*12*, *3*	2c, 2d, 4N
	$2a_1$	1.64, m	40.1	2c, 2d	4N
	$2a_2$	1.53, m			4N
	2b	1.60, m	23.8	2c, 2d	
	2c	0.82, d (6.4)	21.0	2a, 2b, 2d	2
	2d	0.84, d (6.1)	23.0	2a, 2b, 2c	2
	3		**169.4**	**4N-H**, 5, 2	
D-Ala	**4NH**	**8.35**, d (6.8)		*3*	5a, 2, $2a_1$, $2a_2$
	5	4.37, qd (7.3, 6.8)	48.1	5a, 6, *3*	
	5a	1.35, d (7.3)	16.8	5, 6	8
	6		**171.4**	5a, 5, **8**	
L-*O*-Val	**8**	**4.83**, d (4.5)	77.1	8b, 8c, *9*, *6*	8b, 8c, 5a
	8a	2.10, m	30.1	8b, 8c, *9*	10N
	8b	0.80, d (6.8)	16.6	8, 8a, 8c	10N
	8c	0.85, d (6.4)	18.6	8, 8a, 8b	
	9		**168.9**	8, 8a, 11, **10N-H**	
L-Val	**10NH**	**8.03**, d (7.6)		*9*	11a, 11b, 11c, 8, 8a
	11	4.31, dd (7.6, 6.3)	57.7	11a, 11b, 11c, 9, 12	11b, 11c
	11a	2.18, m	29.5	11b, 11c, 11, 12	10N
	11b	0.89, d (6.6)	18.9	11c, 11a, 11	10N, 11
	11c	0.90, d (6.6)	18.1	11b, 11, 11a	10N, 11
	12		**170.5**	11, 11a, **2**	

[a] Recorded at 600 MHz. [b] Recorded at 150 MHz. [c] Proton correlates to carbon resonance in ^{13}C column. Italic numbers represent carbonyl carbon. The assignment was based on the correlations through DQF-COSY, HOHAHA, HMBC and HSQC.

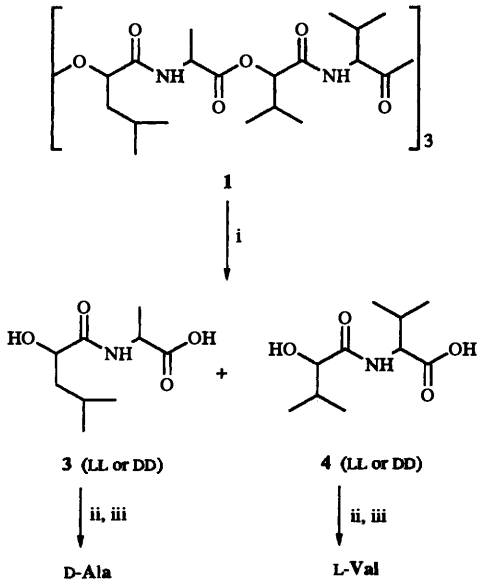

Scheme 1 Hydrolyses of cereulide **1** for the determination of absolute stereochemistry. *Reagents and conditions:* i, KOH, MeOH; ii, H^+; iii, Marfey (ref. 7).

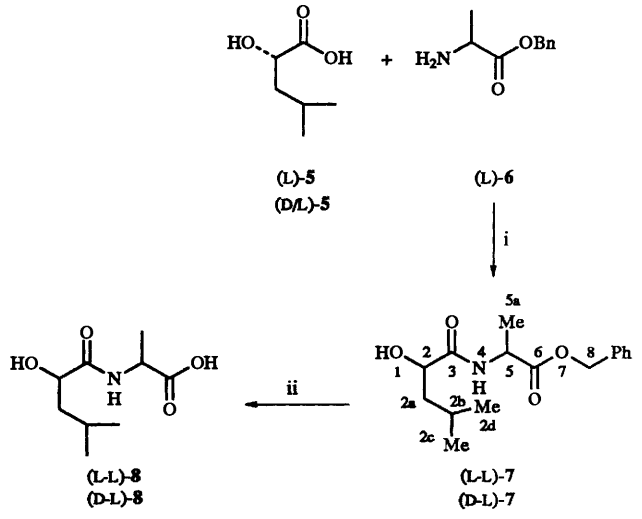

Scheme 2 Synthesis of authentic diastereoisomers of compound **8**. *Reagents:* i, K_2CO_3, DCC; ii, H_2, Pd/C.

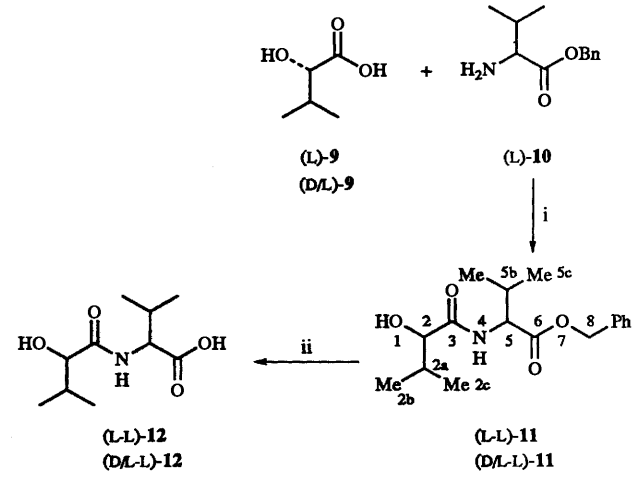

Scheme 3 Synthesis of authentic diastereoisomers of compound **12**. *Reagents:* i, K_2CO_3, DCC; ii, H_2, Pd/C.

(Scheme 1). HPLC analysis of these dipeptides on an ODS column with a gradient of MeCN–water showed that only two peaks eluted, at 14 and 24 min, as illustrated in Fig. 2. The relative stereochemistry of the dipeptides was then determined from the comparison, by HPLC, of retention times with all 4 possible dipeptide diastereoisomers. These diastereoisomers were synthesized from commercially available samples or equivalents (Schemes 2 and 3). The authentic samples eluted with D-*O*-Leu-L-Ala (D-L)-**8** at 11 min, with L-*O*-Leu-L-Ala (L-L)-**8** at 14 min, with D-*O*-Val-L-Val (D-L)-**12** at 16 min and with L-*O*-Val-L-Val (L-L)-**12** at 24 min. The relative configuration of the dipeptides was determined as L-*O*-Leu-L-Ala (or D-*O*-Leu-D-Ala) and L-*O*-Val-L-Val (or D-*O*-Val-D-Val), respectively. The absolute configuration of the amino acid component in each dipeptide was further determined by Marfey's method.[7] Thus,

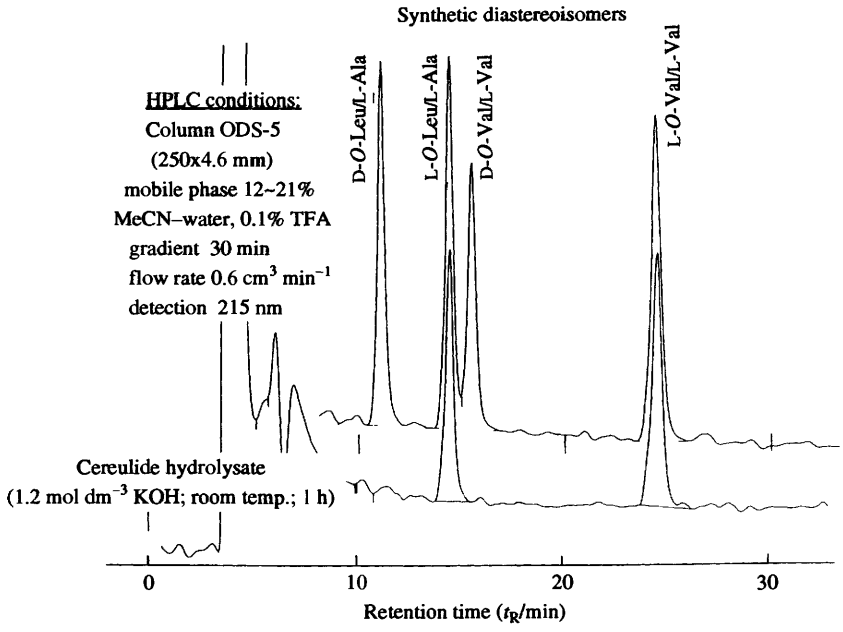

Fig. 2 Comparison of retention times of dipeptide. Top is the chromatogram of four possible diastereoisomers. Bottom is the chromatogram of products of alkali–hydrolysis of cereulide **1**.

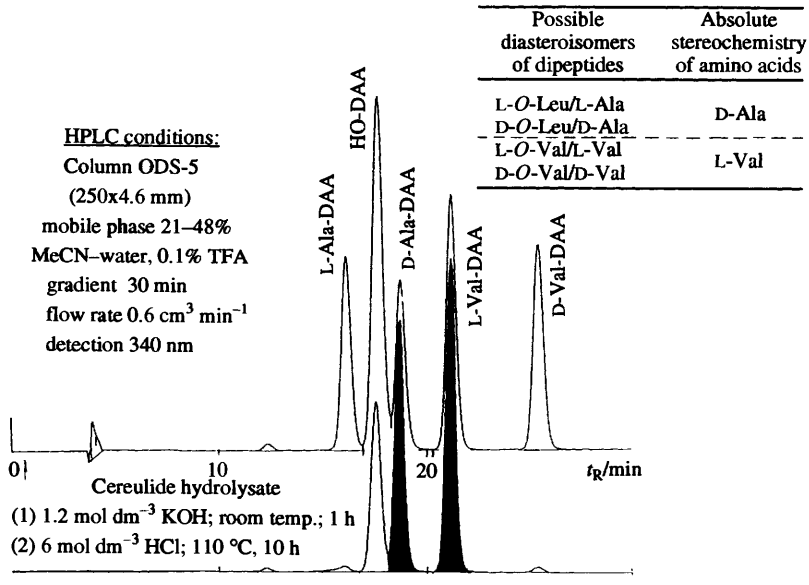

Fig. 3 Comparison of retention times of the L/D-Ala- and L/D-Val-DNP-L-Ala-amide. The chromatogram of the authentic derivatives is on top and that of cereulide amino acid derivatives is on the bottom.

the acid hydrolysate of the mixture of dipeptides **3** and **4** derived from treatment with 6 mol dm^{-3} HCl at 110 °C for 12 h, was then coupled with (5-fluoro-2,4-dinitrophenyl)-L-alaninamide (FDAA) at 40 °C for 1.5 h in the presence of $NaHCO_3$ in acetone. The HPLC peaks of the resultant sample appeared at t_R 18 and 21 min (Fig. 3), and then were compared with the peaks of authentic L/D-Ala-dinitrophenyl(DNP)-L-Ala-NH_2 (16 and 18 min, respectively) and L/D-Val-DNP-L-Ala-NH_2 (21 and 25 min, respectively). Consequently, the absolute stereochemistry of the amino acids obtained from acid hydrolysis of the dipeptide mixture of **1** were D-Ala and L-Val. The stereochemistry of the dipeptide components was therefore concluded to be D-*O*-Leu-D-Ala and L-*O*-Val-L-Val. In conclusion, the complete structure of cereulide was *cyclo*(D-*O*-Leu-D-Ala-L-*O*-Val-L-Val)$_3$. It was optically active $\{[\alpha]_D^{28} -13 \times 10^{-1}$ deg cm^2 g^{-1} (*c* 0.1, $CHCl_3$)$\}$. Its three chemically repeating substructures exhibited the three-fold symmetry in its NMR data.

Characteristics of cereulide and its complexes with alkali metal ions

It is interesting that cereulide **1** possesses the same size of cyclic main chain, the same -L-L-D-D-stereochemistry of alternating amino and oxy acids, and only the same hydrophobic side-chains as valinomycin **2**. These three structural properties theoretically show cereulide to be a new, effectively functioning ionophore similar to the valinomycin group.[8]

In further FAB-MS analyses, the addition of either NaI, KI or CsI to the purest fraction of cereulide made the corresponding $(M + Na)^+$ peak at *m/z* 1175, $(M + K)^+$ peak at *m/z* 1191 or $(M + Cs)^+$ peak at *m/z* 1285 observable, respectively. The FAB-MS spectrum of a cereulide sample from a different lot showed the ion at *m/z* 1191 $(M + K)^+$ as base peak without addition of KI. The addition of NaI to this sample did *not* change the peak of *m/z* 1191 $(M + K)^+$ into that of *m/z* 1175. This meant that the less pure sample had been

Table 2 Chemical shifts and coupling constants of NH and alpha protons of cereulide **1**

Residue	Assignment (multiplicity)	$[^2H_6]$DMSO free [*J* (Hz)]	$CDCl_3$ H^+	Li^+	Na^+	K^+	Rb^+	Cs^+
D-*O*-Leu	2	5.00	5.33	5.31	5.19	4.77	4.78	4.86
	(dd)	(9, 8, 3.5)	(6.8, 6.8)	(8.0, 5.0)	(9.5, 3.4)	(10.0, 3.7)	(9.9, 3.9)	(9.8, 4.0)
D-Ala	4-NH	8.35	7.83	7.79	8.16	8.33	8.12	7.88
	(d)	(6.8)	(7.0)	(6.8)	(4.5)	(4.4)	(4.5)	(4.7)
	5	4.37	4.38	4.36	4.25	4.28	4.24	4.22
	(qd)	(7.3, 6.8)	(7.0, 7.0)	(6.8, 6.8)	(7.1, 4.5)	(7.4, 4.5)	(7.2, 4.5)	(7.2, 4.7)
L-*O*-Val	8	4.83	5.02	5.00	4.98	4.62	4.65	4.72
	(d)	(4.5)	(3.3)	(3.3)	(3.2)	(3.4)	(3.4)	(3.5)
L-Val	10-NH	8.03	7.83	7.79	8.06	8.23	8.03	7.76
	(d)	(7.6)	(~7)	(7.4)	(6.3)	(5.2)	(5.1)	(5.0)
	11	4.31	4.05	4.06	3.86	3.82	3.79	3.79
	(dd)	(7.6, 6.3)	(10.0, 7.3)	(9.9, 7.4)	(10.8, 6.3)	(10.9, 5.2)	(10.7, 5.1)	(10.3, 5.0)

Table 3 Chemical shifts and coupling constants of NH, alpha and beta protons of valinomycin in chloroform

Residue	Assignment (multiplicity)	$CDCl_3$ free [*J* (Hz)]	H^+	Li^+	Na^+	K^+	Rb^+	Cs^+
L-*O*-Ala	2	5.33	5.34	5.31	5.26	4.94	4.94	5.02
	(q)	(6.9)	(6.8)	(6.8)	(7.0)	(7.1)	(7.0)	(7.0)
	2a	1.43	1.43	1.43	1.50	1.54	1.53	1.53
	(d)	(6.9)	(6.8)	(6.8)	(7.0)	(7.1)	(7.0)	(7.0)
L-Val	4-NH	7.80	7.82	7.76	8.13	8.26	8.07	7.86
	(d)	(6.2)	(6.3)	(6.3)	(5.8)	(5.0)	(4.9)	(4.9)
	5	3.96	3.96	3.97	3.82	3.80	3.77	3.74
	(dd)	(10.2, 6.2)	(10.0, 6.3)	(10.1, 6.3)	(11.0, 5.8)	(11.0, 5.0)	(10.9, 4.9)	(10.6, 4.9)
	5a	2.24	2.24	2.23	2.26	2.18	2.19	2.18
	(ds)	(10.2, 6.7)	(10.0, 6.6)	(10.1, 6.6)	(m)	(11.0, 6.6)	(m)	(m)
D-*O*-Val	8	5.01	5.01	5.00	4.99	4.58	4.60	4.67
	(d)	(3.2)	(3.0)	(3.2)	(3.5)	(3.8)	(3.8)	(3.8)
	8a	2.32	2.32	2.33	2.29	2.22	2.19	2.22
	(sd)	(m)	(m)	(m)	(m)	(6.9, 3.8)	(m)	(m)
D-Val	10-NH	7.86	7.87	7.84	8.22	8.37	8.19	7.95
	(d)	(7.9)	(8.0)	(8.0)	(5.6)	(5.0)	(5.0)	(5.0)
	11	4.10	4.10	4.11	3.85	3.84	3.81	3.80
	(dd)	(10.0, 7.9)	(10.0, 8.0)	(9.7, 8.0)	(10.9, 5.6)	(11.0, 5.0)	(10.9, 5.0)	(10.6, 5.0)
	11a	2.33	2.32	2.33	2.26	2.18	2.19	218
	(ds)	(m)	(m)	(9.7, 6.6)	(m)	(11.0, 6.6)	(m)	(m)

contaminated with some K^+ ions and that cereulide did predominantly ionize with K^+ rather than Na^+. This behaviour was similarly observed in the FAB-MS with valinomycin **2**, which gave *m/z* 1111 $(M + 1)^+$, while the addition of either KI, NaI or CsI afforded corresponding peaks at *m/z* 1149.5 $(M + K)^+$, 1133.5 $(M + Na)^+$ or 1243.4 $(M + Cs)^+$, respectively. Addition of a mixture of NaI, KI and CsI, however, showed only *m/z* 1149.5 $(M + K)^+$. This selectivity was strikingly in contrast with that of 18-crown-6. Addition of the three-salts mixture to 18-crown-6 rendered 3 peaks at *m/z* 287 $(M + Na)^+$, *m/z* 303 $(M + K)^+$ and *m/z* 397 $(M + Cs)^+$ observable at the relative intensities of 1:2:1. In this sense, cereulide **1** expressed itself as a potassium-ion selector, as does valinomycin. The complexing ratio of cereulide was thus shown to be 1:1 with either K^+, N^+ or Cs^+.

Five alkali-metal-ion complexes (Li^+, Na^+, K^+, Rb^+, Cs^+) and the H^+ state of cereulide **1** and valinomycin **2** prepared in $CDCl_3$ were comparatively studied by 1D ^1H NMR spectrometry (summarized in Tables 2 and 3). Since the resonances between D- and L-Val of valinomycin **2** could not be specified from 1D ^1H spectral measurements these assignments were based on those reported by Davis and Tosteson.[9]

It is important that the neutral free form of cereulide in $CDCl_3$ gave many ^1H NMR signals with the broad peak shape of NH and α-H signals, and also that the rest of the signals were broad. It indicated that free cereulide possessed many types of conformation in this solvent. As a result, we did not report data for free cereulide in neutral pH and in $CDCl_3$. The sharp signals of cereulide in free form could be obtained in DMSO (Fig. 1). However, when cereulide formed a complex with any alkali metal or was in the free form obtained after shaking the $CDCl_3$ solution with aq. acidic solution (hereafter, we refer to this as the H^+ state or uncomplexed form), all signals became sharp peaks in $CDCl_3$ and assumed three-fold symmetry as well.

The alkali-metal-binding selectivity of cereulide **1** was further studied by NMR data and compared with that of valinomycin **2**. Among the three metal ions, K^+, Na^+ and Cs^+, both cereulide and valinomycin selected only K^+. Moreover, in the mixture of five alkali metal ions only the Rb^+ and K^+ complexes were formed in the ratio 3:1 and 2:1 for cereulide and valinomycin, respectively. These complexed mixtures were concentrated and were further confirmed by FAB-MS; the cereulide sample had the peaks of $(M + Rb)^+$ at *m/z* 1237.5 and $(M + K)^+$ at *m/z* 1191.6 whereas the valinomycin sample showed the peaks of $(M + Rb)^+$ at *m/z* 1195.5 (base peak) and $(M + K)^+$ at *m/z* 1149.5. Thus, cereulide is a rubidium- and potassium-ion-selective ionophore. Similarly, cereulide also formed a 1:1 complex with Rb^+. This result suggested that the Rb^+ and K^+ complexes took highly stable conformations, much more stable than those of the other three alkali-metal

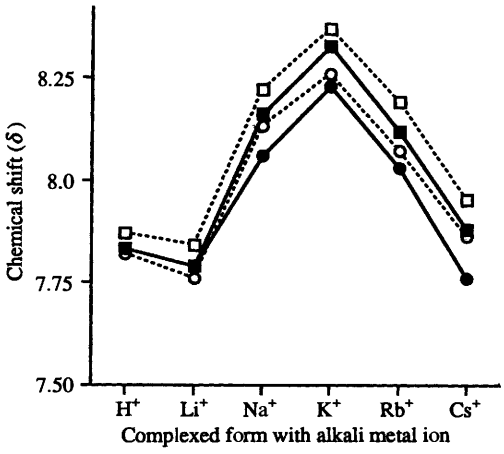

Fig. 4 Changes in chemical shifts of NH protons of cereulide **1** and valinomycin **2**. —●— cereulide–Val; —■— cereulide–Ala; ---○--- valinomycin–Val(1); ---□--- valinomycin–Val(2).

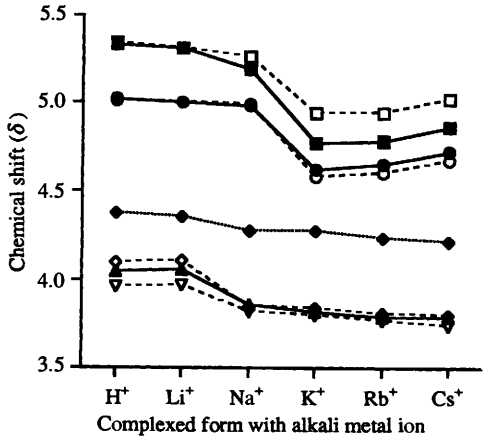

Fig. 5 Changes in chemical shifts of alpha protons of cereulide (C) and valinomycin (V). —■— C-*O*-Leu-2; ····◆···· C-Ala-5; —●— C-*O*-Val-8; —▲— C-Val-11; ---□--- V-*O*-Ala-2; ---◇--- V-L-Val-5; ---○--- V-*O*-Val-8; ---▽--- V-D-Val-11.

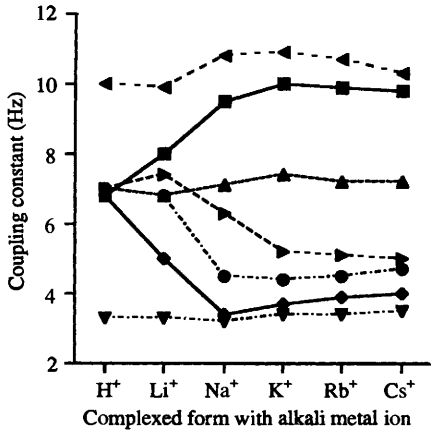

Fig. 6 Changes in coupling constants of cereulide **1** with alkali metal ions. —■— *O*-Leu-αβ1; —◆— *O*-leu-αβ2; –•–●–•– AlaNH; ---▲--- Ala-αβ; –•–▼–•– *O*-Val; ---▶--- ValNH; ---◀--- Val-αβ.

complexes. This also indicated that one of the parameters directly involved in the stability-degree of the ligand conformation was the size of metal ionic radius. The presentation of our NMR data in graphical pattern (Figs. 4–7) thus starts from the uncomplexed (H^+) to the complexed states with the smallest to the biggest radial cations.[10]

In Fig. 4 both NH chemical shift patterns of cereulide Ala and Val showed similar values between the H^+ and Li^+ forms (δ 7.83 and 7.79), changed to higher values in the complexed states with Na^+, K^+ and Rb^+ [becoming the highest with K^+ (δ 8.33 and 8.23)] but dropped down to about the values of the H^+ state with Cs^+ (δ 7.88 and 7.76). This pattern of change suggested that NHs of amino acid residues in the complexed forms must be involved in hydrogen bonding by varying either the strength or number of the hydrogen bonds, or both. Accordingly, NH hydrogen bonding would be maximum (6 NHs) and/or the strongest in the complex with K^+, less in the Na^+ and Rb^+ complexes, and the least in the Cs^+ complex. Considering the size of the respective cationic radii,[10] after cereulide **1** accommodated either K^+ (1.33 Å), Na^+ (0.95 Å) or Rb^+ (1.48 Å) the hydrogen bonds were still strong by some extent, but when it accepted a big ion such as Cs^+ (1.69 Å) or a small cation like Li^+ (0.60 Å) these hydrogen bonds became much looser and/or fewer in number. The most likely atoms to be H^+ acceptors of NH were carbonyl oxygens. Hence, the strengths and numbers of hydrogen bonds with carbonyl oxygens were the parameters affected by the cation.

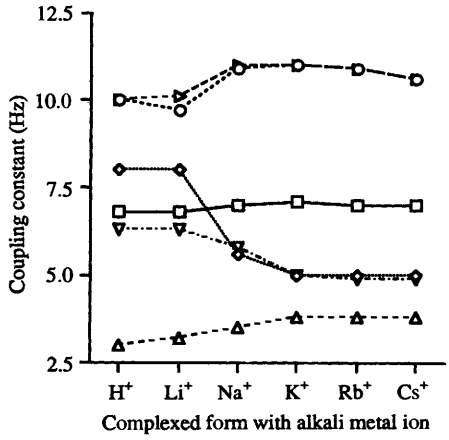

Fig. 7 Changes in coupling constants of valinomycin **2** with alkali metal ions. —□— *O*-Ala; ---◇--- D-Val-NH; ---○--- D-Val-αβ; ---△--- *O*-Val; –•–▽–•– L-Val-NH; ---▷--- L-Val-αβ;

Other important chemical shifts are those of alpha protons which directly link to the arrangement of the main ring chain. As shown in Fig. 5 the alpha protons of cereulide D-Ala and L-Val changed in a very similar manner and the changes in value of their chemical shifts are rather small for all forms of complexation. This is in contrast with the alpha protons of the oxy acids. Both alpha protons of oxy acids (D-*O*-Leu and L-*O*-Val) also have the same pattern of change. However, the δ-values of these alpha protons in the H^+–Li^+–Na^+ complex group are between δ 5.33 and 4.98 while those in the K^+–Rb^+–Cs^+ complex group are between δ 4.86 and 4.62. The difference in value between these two groups (min. 0.26 ppm) appeared very clearly. Hence, this characteristic may tell us that in the K^+ and Rb^+ complexes alpha protons of oxy acids might stay in a closer position than in the Cs^+ complex because of the higher chemical shift induced by the cations. Similarly, the two oxy alpha protons might stay further from its cation in the Li^+ and Na^+ complexes as there was much less or no effect from the cation compared with the uncomplexed state. We propose further that the alpha protons of oxy acids might turn toward the inside of the ring. On the other hand, the alpha protons of amino acid residues, showing no such difference though also on the main chain, may have their orientation toward the outside of the ring.

Based on all the above considerations we infer for the conformation of the cereulide–alkali metal complexes that the cation should be situated in the centre of the cavity by means of ion–dipole bonds with some of carbonyl groups, the backbone

Table 4 ^{1}H NMR data of the cereulide–K^+ complex in $CDCl_3$

Residue	Assignment	δ_H(mult)	J (Hz)	Calc.[a] J	Dihedral angle[a]	NOESY	NOE Distance[a] (Å)
D-*O*-Leu	2	4.76, dd	10.0, 3.7	11.7, 2.4	175 ($2a_1$) 59 ($2a_2$)	2b, 2c 4N, 11a	3.24, 2.38 3.41, 2.85
	$2a_1$	1.84, ddd	14.3, 10.0, 4.3	11.7, 2.6	175 (2) 64 (2b)	2d	2.49
	$2a_2$	1.63, m		12.4	−179 (2b)	2c, 2d	2.62, 2.64
	2b	1.74, m				2	3.24
	2c	0.87, d	6.5			2, $2a_2$	2.38, 2.62
	2d	0.95, d	6.7			$2a_1$, $2a_2$	2.49, 2.64
D-Ala	4N	8.32, d	4.4	6.2	135 (5)	5a, 2, 11	2.50, 3.41, 3.62
	5	4.27, qd	7.3, 4.4	6.2	135 (4N)	8b, 8c, 10N	3.67, 3.85, 3.67
	5a	1.47, d	7.3			4N, 8, 8b, 8c	2.50, 2.57, 3.59, 3.50
L-*O*-Val	8	4.61, d	3.3	1.5 (2.6)[b]	−62 (8a) (62)[b]	8b, 8c, 5a, 10N (8b, 8c)[b]	3.83, 2.50, 2.57, 3.36 (3.82, 2.49)[b]
	8a	2.30, sd	6.9, 3.3				
	8b	0.99, d	6.9			8, 5, 5a, 10N	3.83, 3.67, 3.59, 4.94
	8c	1.15, d	6.9			8, 5, 5a, 10N	2.50, 3.67, 3.50, 3.43
L-Val	10N	8.22, d	5.2	6.7	−140 (11)	11a, 11c, 5, 8, 8b, 8c	2.48, 2.42, 3.67, 3.36, 4.94, 3.43
	11	3.82, dd	10.9, 5.2	11.4, 6.7	178 (11a), −140	11b, 11c, 4N	2.60, 2.62, 3.62
	11a	2.24, ds	10.9, 6.6	11.4	178 (11)	10N, 2	2.48, 2.85
	11b	0.93, d	6.8			11	2.60
	11c	1.12, d	6.4			10N, 11	2.42, 2.62

[a] Obtained from the molecular mechanics calculation by BioGraf using Dreiding force field energy calculation and by MacroModel for J-values. See Experimental section for details. [b] Relating to the other conformation of L-*O*-Val side-chain in the 25% population, NOE distance (Å): 5–8b (5.70), 5–8c (3.88), 5a–8b (2.89), 5a–8c (5.52), 8–8b (3.82), 8–8c (2.49), 8b–10N (4.69), 8c–10N (3.22).

must orient in such a way as to enable the size of the central cavity just to fit well with only Rb^+ and K^+, forming highly stable complexes, and at the same time turning the oxy acid alpha protons inwards the cavity but the amino acid alpha protons outwards. Moreover, in the case of the K^+ complex the backbone has shortened and symmetrically arranged until it allows the NH protons to form the maximum (6) or/and the strongest hydrogen bonds with the carbonyl oxygens, but in the cases of the other cation complexes or the uncomplexed state the cation cannot make the backbone rearrange sufficiently so that all or some of NH- -O=C hydrogen bonds may become weaker or loose. Consequently, the net sum of the numbers and strengths of NH hydrogen bonds of cereulide complexes were seen to be in the order $K^+ > Na^+ > Rb^+ > Cs^+ > H^+, Li^+$ (Fig. 4).

The J-values of cereulide HN–Hα and Hα–Hβ are shown in Fig. 6. The most prominent J-value which varied much according to the guest metal ion are the Js of Hα–Hβ1 and Hα–Hβ2 of *O*-Leu. The bigger J (Hα–Hβ1) of the complexed forms varied between 10.0 and 8.0 Hz while the smaller J (Hα–Hβ2) varied between 5.0 and 3.4 Hz. The difference in value of these two Js appeared similarly in the four Cs^+, Rb^+, K^+ and Na^+ complexes but became less in the Li^+ form. These two Js became identical (6.8 Hz) in the H^+ state. These data clearly indicated that the side-chain of *O*-Leu had freely rotated in the uncomplexed state but existed in certain conformations in the complexed forms. The HN–Hα coupling constants of both D-Ala and L-Val residues exhibited distinct values between the H^+–Li^+ group (6.8–7.4 Hz) and the K^+–Rb^+–Cs^+ group (4.4–5.2 Hz). These two J-values were different in the Na^+ complex. Its L-Val HN–Hα coupling constant was in the middle value between the two aforementioned groups. This suggests that the orientation of NHs of the K^+, Rb^+ and Cs^+ complexes was allowed at only certain angles so that this complex group still have similar conformations of the main chain. The NHs of D-Ala and L-Val of the H^+–Li^+ group had free rotation. Consequently, the H^+ state and the Li^+ complex should have less chance for formation of H-bonds. In addition the orientation of NHs of L-Val residue(s) in the Na^+ complex was less appropriate to the formation of H-bonds than that of Ala residues. Thus, the main chain conformation of the Na^+ complex resulting from some H-bonds should be an intermediate conformer between the highly stable complexes (the K^+ and Rb^+) and the unstable complex (the Li^+). The Hα–Hβ coupling constants of L-*O*-Val in all forms (3.2–3.5 Hz) were comparable and those of D-Ala were between 7.4 and 6.8 Hz. The J-values between HN–Hα of L-Val varied between 5.0 and 7.4 Hz, while its Hα–Hβ coupling constants were between 10.9 and 9.9 Hz. In conclusion, these J-data indicated that the main-chain conformations of the Cs^+, Rb^+, K^+ complexes were similar but those of the Li^+ and uncomplexed forms arranged in a different way and that of the Na^+ complex was intermediate between these two groups.

Higher structure of the cereulide–K^+ complex

There was a difference in some of the atomic proximity-through-space (NOE) data between the NOE in a rotating frame (ROESY) signals of the natural cereulide measured in DMSO (Table 1) and the NOESY signals of the cereulide–K^+ complex in $CDCl_3$ (Table 4). The NOE found in DMSO showed fewer interresidual NOEs (6) and these NOEs provided the same unambiguous conclusion about sequential connectivity as the HMBC data did. More interresidual NOEs of the K^+ complex were found in $CDCl_3$ (16) and not only between the sequential residues. These directly indicate the difference in their conformations.

It is also important to mention that all parameters that we examined with cereulide, which are chemical shifts of NH and α protons (Figs. 4 and 5) and the Js of HN–Hα and Hα–Hβ (Fig. 6), except the Js of *O*-Leu, showed very similar patterns of changes with the corresponding residues existing in valinomycin (Figs. 4, 5 and 7). The results of our studies on proton chemical shifts (Figs. 4 and 5) and vicinal coupling constants of valinomycin

and its cation complexes in $CDCl_3$ (Fig. 7) agreed well with those studies by Davis and Tosteson.[9] These have confirmed that our interpretation of the conformations of the cereulide complexes based on the proton NMR data is not incorrect and at the same time some known important details about valinomycin conformation (confirmed by X-ray crystallographic analysis[11]) could be applied to cereulide as well. Accordingly, we had taken two main characteristics of the valinomycin–K^+ complex about the 6-ion-dipole bonds between K^+ situated centrally and the ester carbonyl turning inwards plus 6 strong intramolecular 4→1 β-turn hydrogen bonds between all 6 NHs and amide carbonyl oxygens[11-13] in computing a local minimum-energy conformation[14] of the cereulide–K^+ complex. Consequently, a hexagonal cylinder-like structure of the main chain (which is similar to the known bracelet-like structure in valinomycin[13]) was automatically obtained from molecular mechanics calculations and after additional refinement of the side-chain conformation by the computed data (presented in Fig. 8a–c and Table 4) the proposed conformation still had minimum energy and three-fold symmetry for the whole molecule. The calculated *J*-values of the proposed K^+ complex showed no objection against the experimental data (Table 4). These values, for the molecule in the local minimum energy, were confirmed by sequential searching through varying the dihedral angle C(=O)–Cα–Cβ–Cγ (and the dihedral angle Cα–Cβ–Cγ–Hγ in the case of *O*-Leu) in every 5° (Fig. 8a–c). The conformation of D-*O*-Leu side-chain (Fig. 8a) with dihedral angle C(=O)–Cα–Cβ–Cγ 180° corresponding to the proton–proton coupling constants 11.7, 2.4 Hz had the lowest energy lower than that with the same dihedral angle 55° corresponding to the *J*-values 3.3, 3.1 Hz by 1.2 kcal mol^{-1}.† The dihedral angle Cα–Cβ–Cγ–Hγ 300° corresponding to proton–proton *J*s 12.4, 2.6 Hz gave another correlating minimum-energy conformer. Thus, the combination of these two minimum-energy conformers were adopted for the proposed conformation of the *O*-Leu side-chain. For the L-Val side chain (Fig. 8b), the lowest-energy conformation having a dihedral angle 300° (corresponding to a proton–proton *J* 11.4 Hz) was given. The different conformations of the major and minor population had to be considered in the case of L-*O*-Val side-chain (Fig. 8c). The two conformers possessing the dihedral angles 55° and 180° (corresponding to calculated *J*-values of 1.5 and 2.6 Hz, respectively) were possible side-chain conformers of L-*O*-Val in 75% and 25% of the total population, respectively. Because their relative energy difference was only 0.65 kcal mol^{-1} (63.74 and 64.39 kcal mol^{-1}). All the experimental *J* and NOE data had conformity with their corresponding calculated *J*, dihedral angle and distance data (Table 4) measured from our proposed K^+ complex models. The found NOEs between the pairs of *O*-Leu Hα–Val Hβ and Ala NH–*O*-Val Hα are clear evidence supporting the proposed model.

The schematic illustrations of the K^+ complex are presented in Fig. 9. Looking at the details of this model, we found that the backbone arranged in such a way as to leave the frame as a hexagonal cylinder-like structure. The guest K^+ ion is centrally situated in the cavity (not shown). An alpha C of every residue is located at every corner. Each horizontal side of the hexagonal cylinder consists of 4 atoms of the main chain in the pattern of –Cα–O–C(=O)–Cα– whereas each vertical side consists of –Cα–N–C(=O)–Cα–. This arrangement provided the chance for NH– –O=C hydrogen bonds to occur easily between the neighbouring vertical chains so this cylinder is wrapped around along the *Y*-axis by 6 hydrogen bonds in 2 different horizontal levels. The ester carbonyl on the horizontal plane points inwards, thus leaving 3 carbonyl oxygens of L-Val on the top plane of the cylinder and the other 3 carbonyl oxygens, of D-Ala, on the bottom plane and all of them have ion–dipole interactions with the K^+. All 6 oxy acid alpha protons pointed inwards from the top and bottom planes while the other 6 amino acid alpha protons turned outwards. This can explain the unequal effects of the cation on the chemical shifts of oxy and amino acid alpha protons. A stereoview of the cereulide–K^+ complex are given in Fig. 10.

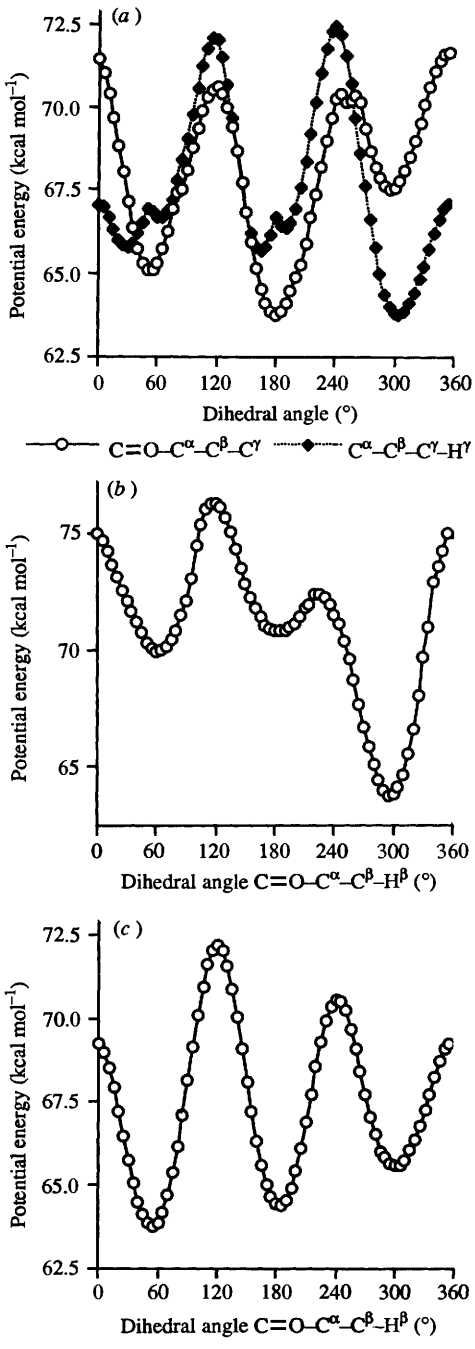

Fig. 8 (*a*) Energy plot of rotation around C^{α}–C^{β} and C^{β}–C^{γ} bonds of D-*O*-Leu. (*b*) Energy plot of rotation around C^{α}–C^{β}– bond of L-Val. (*c*) Energy plot of rotation around C^{α}–C^{β} bond of L-*O*-Val.

Our understanding of the cereulide–K^+ complex has allowed us to extend our interpretation to the conformations of the considerably less stable complexes such as the Li^+ form and the uncomplexed state. The conformations of those states may be as follows: The frameworks of their main chain might lose its compactness, becoming more linearly extended, which results in

† 1 cal = 4.184 J.

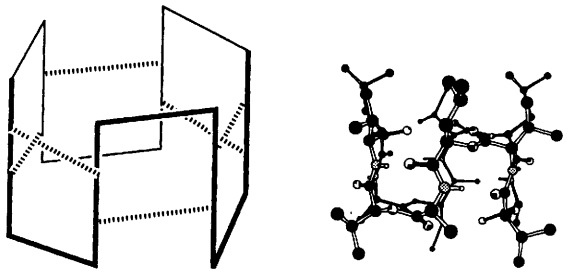

Fig. 9 A hexagonal cylinder-like framework of the main chain of the cereulide K^+ complex

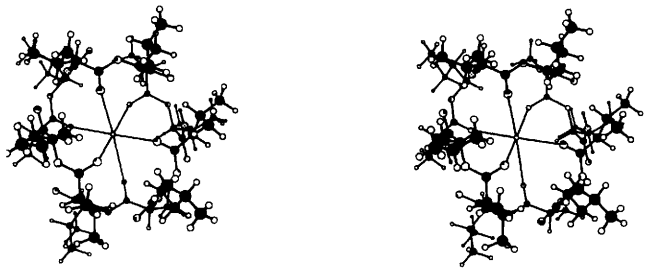

Fig. 10 A stereo pair of the cereulide-K^+ complex

a bigger cavity diameter, fewer hydrogen bonds could be formed, and all the residual side-chains could freely rotate. The conformation(s) of the Na^+ complex might take an intermediate conformer between those of the highly and less stable complexes.

It is interesting that the K^+-selective binding property of cereulide may primarily be the cause of not only its activity in forming vacuoles, which was recognized as the swelling of mitochondria in an HEp-2 cell,[15] but also its emetic activity.

Experimental

Cereulide was isolated and purified according to the method described by Agata *et al.*[5] The amount available for structure elucidation studies was in the 200 μg range. Later, another sample (~2 mg) was obtained for an optical-rotation measurement and complexation studies. $[\alpha]_D^{28}$ -13×10^{-1} deg cm^2 g^{-1} (*c* 0.1, $CHCl_3$). Valinomycin was obtained from Molecular Probes, Inc., USA.

General procedures

Optical rotation was measured on a JASCO DIP-370 digital polarimeter. HPLC was performed on a JASCO Gulliver system composed of two PU-980 pumps, an UV-970 UV/VIS detector and an 807-IT integrator. The system was equipped with a Develosil ODS-5 column (4.6 × 250 mm). All FAB-MS analyses were recorded on a JEOL JMS-DX 705L spectrometer using *m*-nitrobenzyl alcohol as matrix. Solutions of NaI, KI and CsI (~0.1 mol dm^{-3}) in acetone were used as additives to the matrix for measurement of the ion-selective behaviour. NMR spectra for the structure elucidation were recorded at 27 °C on a Bruker AMX-600 spectrometer, operating at 600 and 150 MHz for ^1H and ^{13}C, respectively. The sample (~100 μg) was prepared in [$^2H_6$]DMSO solvent and in a reduced-volume NMR sample tube (Shigemi Standard Joint Ind. Co. Ltd., cat. # BMS-005, 5 mm diam.). 1D-^1H and ^{13}C NMR plus 2D-NMR experiments of DQFCOSY, HOHAHA, ROESY, HSQC and HMBC were measured. Two HMBC experiments were performed to measure coupling signals of 10 and 5 Hz. The residual protio–deuterio solvent signal was referenced at δ 2.49 for proton spectra. The ^{13}C signal of DMSO was referenced at δ_C 39.5. *J*-values are in Hz. The proposed conformational modelling was processed on a SiliconGraphics Power Iris 220GTXB computer using Biograf program version 3.21 (Molecular Simulations, Inc.) and Dreiding-II force-field energy calculations.[14] The *J*-value was calculated by MacroModel version 4.

Syntheses of L-*O*-Leu-L-Ala benzyl ester (L-L)-7 and L-*O*-Leu-L-Ala (L-L)-8 (Scheme 2)[16]

L-Alanyl benzyl ester·HCl **6** (221 mg, 1.02 mmol, Sigma) in water (0.8 cm^3) was treated with K_2CO_3 (0.4 cm^3, 1.44 mmol) in a vial in an ice–water-bath. The mixture was extracted with diethyl ether (2.5 cm^3; three times). The extracts were combined, dried over $MgSO_4$, and filtered through cotton wool. The solvent was evaporated off and the mixture was evacuated. The residue (163 mg, 0.91 mmol) was totally transferred to a 10 cm^3 flask by a small volume of dichloromethane. L-(−)-2-Hydroxy-4-methylpentanoic acid (L-*O*-Leu) (L)-**5** (59.5 mg, 0.45 mmol, Aldrich) was added to the flask to adjust the final volume of dichloromethane to ~2 cm^3. Then dicyclohexylcarbodiimide (DCC) (92.8 mg, 0.45 mmol, Nacalai tesque) was added. Precipitation occurred after the addition of DCC. After being continuously stirred at room temp. (15 °C) for 1.5 h, the whole mixture was filtered through cotton wool to remove the precipitate. The mixture was separated on a silica gel column equilibrated with (4:1) hexane–diethyl ether. Elution conditions by the solvent mixture were (80:20) (100 cm^3), (60:40) (100 cm^3), (40:60) (200 cm^3) and (40:80) (120 cm^3), successively. The desired compound was obtained in the fractions of (40:60) hexane–diethyl ether. The amount of pure dipeptide benzyl ester (L-L)-7 obtained was 28.1 mg (0.10 mmol, 75%) after evaporation of the solvent and evacuation. Its silica gel TLC plate developed twice with (2:1) diethyl ether–hexane showed a spot at R_f 0.36. (L-L)-7 had δ($CDCl_3$; 270 MHz) 0.93 (3 H, d, *J* 6.5, Me2c), 0.94 (3 H, d, *J* 6.5, Me2d), 1.42 (3 H, d, *J* 7, Me5a), 1.57 (2 H, m, H2a), 1.87 (1 H, m, H2b), 3.29 (1 H, d, *J* 5, OH), 4.15 (1 H, m, H2), 4.63 (1 H, quint, *J* 7.5, H5), 5.18 (2 H, AB, H8), 7.11 (1 H, d, *J* 7.5, NH) and 7.34 (5 H, s, Ph).

L-*O*-Leu-L-Ala benzyl ester (L-L)-7 (10.3 mg, 0.035 mmol) was dissolved in a mixture of (7:2:1) ethanol–water–acetic acid (1 cm^3) under N_2. Then 10% palladium-on-charcoal (5 mg) was added. The reaction mixture was stirred under H_2 for 5 h at room temp. (15 °C), and then the catalyst was removed by filtration through cotton wool and washed with a small volume of the solvent. The combined solution was evaporated and evacuated. The amount of dipeptide was quantitative, (L-L)-**8** δ_H($CDCl_3$; 270 MHz) 0.92 (3 H, d, *J* 7, Me2c), 0.95 (3 H, d, *J* 7, Me2d), 1.45 (3 H, d, *J* 7, Me5a), 1.54 (2 H, m, H2a), 1.85 (1 H, m, H2b), 4.15 (1 H, dd, *J* 8 and 4.5, H2), 4.49 (1 H, br quint, *J* 7, H5), 5.18 (2 H, AB, H8) and 7.34 (1 H, d, *J* 6.5, NH). FAB-MS (pos. 3-nitrobenzyl alcohol) *m*/*z* 204 (M + H), 226 (M + Na) and 248 (M − H + 2Na).

Syntheses of D-*O*-Leu-L-Ala benzyl ester (D-L)-7 and D-*O*-Leu-L-Ala (D-L)-8 (Scheme 2)

Same procedures and similar scales of starting materials as described for L-*O*-Leu-L-Ala (L-L)-**8** were applied. Thus, only the differences are described. Racemic 2-hydroxy-4-methylpentanoic acid (D/L)-**5** (69 mg, 0.52 mmol, Aldrich) was coupled with L-Ala benzyl ester. Pure D-*O*-Leu-L-Ala benzyl ester (D-L)-7 was obtained in the later fractions of (40:60) hexane–diethyl ether than in the case of L-*O*-Leu-L-Ala benzyl ester diastereoisomer (L-L)-7. Its TLC spot appeared at R_f 0.29. The amount of pure D-*O*-Leu-L-Ala benzyl ester (D-L)-7 was 16.8 mg (0.057 mmol, 11%) and was totally used for the subsequent debenzylation. D-*O*-Leu-L-Ala (D-L)-**8** was thus obtained (10 mg, 85%). (D-L)-7 δ_H($CDCl_3$; 270 MHz) 0.96 (6 H, d, *J* 6.5, Me2c,2d), 1.44 (3 H, d, *J* 7, Me5a), 1.58 (2 H, m, H2a), 1.84 (1 H, m, H2b), 2.45 (1 H, d, *J* 5, OH), 4.16 (1 H, m, H2), 4.65 (1 H,

quint, *J* 7.3, H5), 5.18 (2 H, AB, H8), 6.95 (1 H, d, *J* 7, NH) and 7.35 (5 H, s, Ph). (D-L)-**8** δ_H(CD_3OD; 400 MHz) 0.94 (6 H, d, *J* 6.8, Me2c,2d), 1.42 (3 H, d, *J* 7.1, Me5a), 1.53 (2 H, m, H2a), 1.86 (1 H, m, H2b), 4.05 (1 H, dd, *J* 9 and 5, 2-H) and 4.40 (1 H, q, *J* 7.0, H5). FAB-MS (pos. 3-nitrobenzyl alcohol) *m/z* 204 (M + H), 226 (M + Na) and 248 (M − H + 2Na).

Syntheses of L-*O*-Val-L-Val benzyl ester (L-L)-11 and L-*O*-Val-L-Val (L-L)-12, DL-*O*-Val-L-Val benzyl ester (D/L-L)-11 and DL-*O*-Val-L-Val (D/L-L)-12 (Scheme 3)

L-Val benzyl ester·HCl L-**10** (Sigma), (*S*)-(+)-2-hydroxy-3-methylbutyric acid (L-*O*-Val) L-**9** (Aldrich) and (±)-2-hydroxy-3-methylbutyric acid (DL-*O*-Val) (D/L)-**9** (Aldrich) were used. After the peptide bond had formed (5 h) at room temp. the mixtures were stored at −30 °C for 1 day [(L-L)-**11**] and 2 days [(D/L-L)-**11**] until the subsequent steps were processed. The two benzyl ester diastereoisomers coeluted in the same fractions of (40:60) hexane–diethyl ether and the TLC spots showed the same R_f-value of 0.37. Amounts of pure L-*O*-Val-L-Val benzyl ester (L-L)-**11** and DL-*O*-Val-L-Val benzyl ester (D/L-L)-**11** were 31.8 mg (0.103 mmol, 21%) and 46.2 mg (0.15 mmol, 29%), respectively. The starting amount of L-*O*-Val-L-Val benzyl ester (L-L)-**11** for cleavage of the benzyl group was 12.8 mg (8 mg catalyst; 10 h reaction time) and L-*O*-Val-L-Val (L-L)-**12** was obtained in quantitative yield.

DL-*O*-Val-L-Val benzyl ester (D/L-L)-**11** was used (21.6 mg) in the same cleavage step (13 mg catalyst; 10 h reaction time) and DL-*O*-Val-L-Val (D/L-L)-**12** was obtained in quantitative yield. (L-L)-**11** δ_H($CDCl_3$; 270 MHz) 0.87 (6 H, d, *J* 6.8, Me2b,2c*), 0.93 (3 H, d, *J* 6.8, Me5b*), 1.03 (3 H, d, *J* 6.8, Me5c*), 2.19 (2 H, m, H2a,5a), 4.01 (1 H, d, *J* 3.2, H2), 4.62 (1 H, dd, *J* 9 and 3.2, H5), 5.17 (2 H, AB, H8), 7.04 (1 H, d, *J* 9, NH) and 7.35 (5 H, s, Ph) (* interchangeable). (L-L)-**12** δ_H($CDCl_3$; 270 MHz) 0.87 (3 H, d, *J* 6.8, Me2b*), 0.94 (3 H, d, *J* 6.8, Me2c*), 0.98 (3 H, d, *J* 6.8, Me5b*), 1.02 (3 H, d, *J* 6.8, Me5c*), 2.12 (1 H, m, H2a#), 2.27 (1 H, m, H5a#), 4.01 (1 H, d, *J* 3.5, H2), 4.46 (1 H, dd, *J* 8.5 and 4.5, H5) and 7.28 (1 H, d, *J* 8.5, NH). FAB-MS (pos. 3-nitrobenzyl alcohol) *m/z* 218 (M + H), 240 (M + Na) and 262 (M − H + 2Na) (*, # interchangeable).

(D-L)-**11** δ_H($CDCl_3$; 270 MHz) 0.87 (3 H, d, *J* 6.8, Me2b*), 0.87 (3 H, d, *J* 6.8, Me2c*), 0.92 (3 H, d, *J* 6.8, Me5b*), 1.03 (3 H, d, *J* 6.8, Me5c*), 4.03 (1 H, d, *J* 3.0, H2), 4.61 (1 H, dd, *J* 9 and 4.5, H5), 5.17 (2 H, AB, H8), 6.88 (1 H, d, *J* 9, NH) and 7.35 (5 H, s, Ph). Signals were read from above mixture of diastereoisomers (* interchangeable). (D-L)-**12** δ_H($CDCl_3$; 270 MHz) 0.87 (3 H, d, *J* 6.8, Me2b*), 0.95 (3 H, d, *J* 6.8, Me2c*), 0.98 (3 H, d, *J* 6.8, Me5b*), 1.02 (3 H, d, *J* 6.8, Me5c*), 4.05 (1 H, d, *J* 3.5, H2), 4.50 (H5, overlapped with L-L diastereoisomer) and 7.14 (1 H, d, *J* 8.0, NH). Signals were read from a mixture of diastereoisomers (* interchangeable). FAB-MS (pos. 3-nitrobenzyl alcohol) *m/z* 218 (M + H), 240 (M + Na) and 262 (M − H + 2Na).

Comparison of the dipeptides 3 and 4 derived from cereulide 1 with synthetic dipeptides

Dry cereulide (~100 μg) was dissolved in methanol (300 mm^3). A fraction (10 mm^3) was mixed with 1.2 mol dm^{-3} KOH (50 mm^3) at room temp. (15 °C). Each aliquot (10 mm^3) of this mixture was sampled at 30 and 75 min after mixing, and was neutralized by the addition of 10% TFA (9 mm^3), before HPLC analysis. The four synthesized dipeptides (L-L)-**8**, (D-L)-**8**, (L-L)-**12** and (D-L)-**12** were semiquantitatively diluted with 30% acetonitrile–water and they were used as standard dipeptides for comparison of retention times. These four standard dipeptides and the alkali hydrolysate of cereulide were compared by HPLC retention times on a Develosil ODS-5 column (4.6 × 250 mm) by a linear gradient of 12–21% MeCN–water containing 0.1% TFA for 30 min at a flow rate of 0.6 cm^3 min^{-1}. The chromatogram was monitored at 215 nm. Results are shown in Fig. 2.

Absolute stereochemistry of Ala and Val of cereulide 1

Synthesis of FDAA and derivatization of D- and L-amino acids by FDAA were carried out following the procedures described by Marfey.[7] Four authentic amino acids, D- and L-Ala and D- and L-Val, were prepared in 50 mmol dm^{-3} concentration in water.

Dry cereulide (~100 μg) placed in a small, long, glass tube was first hydrolysed with 1.2 mol dm^{-3} KOH (100 mm^3) at 50 °C for 2 h. The hydrolysate was neutralized with 6 mol dm^{-3} HCl (20 mm^3) and evaporated to dryness. It was then subjected to acid hydrolysis with 6 mol dm^{-3} HCl (100 mm^3) at 110 °C for 12 h. After cooling, only the solution portion was transferred to a 1.5 cm^3 plastic microcentrifuge tube. This acid hydrolysate was evaporated to dryness under reduced pressure. The acid-free sample was redissolved in water (25 mm^3) before derivatization with FDAA as described below.

Each aliquot (25 mm^3, 1.25 μmol) of the authentic amino acid solution or sample was mixed with 1% FDAA in acetone (50 mm^3) and 1 mol dm^{-3} aq. $NaHCO_3$ (10 mm^3). The contents were incubated at 40 °C for 1.5 h with occasional mixing. After cooling to room temperature, the mixture was neutralized with 2 mol dm^{-3} HCl (5 mm^3). This stock solution was 80–85-fold diluted with methanol and aliquots (10 mm^3) were used for injection. Water was used as reagent blank.

The HPLC conditions for the D- and L-amino acid derivatives on a Develosil ODS-5 column (4.6 × 250 mm) were a linear gradient of 21–48% MeCN–water containing 0.1% TFA for 30 min at a flow rate of 0.6 cm^3 min^{-1}. The chromatogram was monitored at 340 nm and is shown in Fig. 3.

Complexation with alkali metal ions and decomplexation for NMR studies

Concentrations of cereulide and valinomycin in $CDCl_3$ for these studies were ~0.3 and 1.5 mmol dm^{-3} respectively. Alkali metal salts used were NaSCN, KSCN, CsF, $NaNO_3$, KNO_3, $CsNO_3$, $LiNO_3$ and $RbNO_3$. The solution of 0.1% TFA in water was used to recover the uncomplexed (H^+) state. The sample solution of deuteriated chloroform (0.6 cm^3) was shaken with saturated alkali salt solution(s) (0.1 cm^3) or 0.1% TFA, then only the chloroform layer was filtered through cotton wool before being transferred to an NMR sample tube. One-dimensional proton NMR spectra of cereulide and valinomycin complexes were recorded on the same 600 MHz spectrometer, using the $CHCl_3$ signal as reference at δ_H 7.24. Another fraction of cereulide (2 mg) was prepared in the K^+-complexed form by using KNO_3 in a similar way to that just described so that the concentration was 2.9 mmol dm^{-3}. The proton 1D and 2D modes including HOHAHA and NOESY were measured for this sample in order to obtain additional data on the cereulide–K^+ complex (presented in Table 4).

Computer modelling of the cereulide–K^+ complex

One favourable conformation of the cereulide molecule without hydrogen atoms was searched for and selected on the basis of the lowest energy obtained after minimization. Then, the distance constraints were used between the centroid situated in the centre of the ring and each of the six carbonyl oxygens of the amino acid residues which undergo coordination, and the energy was minimized. All protons were then attached to the lowest-energy conformation obtained above, and minimized. The distance constraints were again used between all NHs and carbonyl oxygens of oxy acid residues in order to calculate hydrogen bondings. After minimization, the structures of the side-chains were refined by the calculated dihedral angles obtained from the sequential searching of the dihedral angle C(=O)–Cα–Cβ–Cγ

rotating from 0° to 360° in steps of 5°, followed with minimization (Fig. 8a–c). The corresponding distance between H–H atoms of those giving NOE effects in the experimental data (Table 4) was measured and is presented in Table 4.

Acknowledgements

We acknowledge financial support by a Grant-In-Aid for Scientific Research from the Ministry of Education, Science and Culture, Japan. One of the authors (S. S.) expresses her sincere gratitude for a scholarship from the Hitachi International Scholarship Foundation. Thanks are also given to Mr. Shigeyuki Kitamura of the School of Agricultural Sciences, Nagoya University for high-resolution and regular FAB-MS measurements.

References

1 J. Melling, B. J. Capel, P. C. B. Turnbull and R. J. Gilbert, *J. Clin. Pathol.*, 1976, **29**, 938.
2 J. Melling and B. J. Capel, *FEMS Microbiol. Lett.*, 1978, **4** 133.
3 P. C. B. Turnbull, J. M. Kramer, K. Jorgensen, R. J. Gilbert and J. Melling, *Am. J. Clin. Nutr.*, 1979, **32**, 219.
4 R. A. Szabo, J. I. Speirs and M. Akhtar, *J. Food Prot.*, 1991, **54**, 272.
5 N. Agata, M. Mori, M. Ohta, S. Suwan, I. Ohtani and M. Isobe, *FEMS Microbiol. Lett.*, 1994, **121**, 31.
6 S. Hughes, B. Bartholomew, J. C. Hardy and J. M. Kramer, *FEMS Microbiol. Lett.*, 1988, **52**, 7.
7 P. Marfey, *Carlsberg Res. Commun.*, 1984, **49**, 591.
8 Yu. A. Ovchinnikov, *FEBS Lett.*, 1974, **44**, 1.
9 D. G. Davis and D. C. Tosteson, *Biochemistry*, 1975, **14**, 3962.
10 F. A. Cotton and G. Wilkinson, *Advanced Inorganic Chemistry*, Wiley, New York, 4th edn., 1980, p. 14.
11 K. Neupert-Laves and M. Dobler, *Helv. Chim. Acta*, 1975, **58**, 432.
12 M. Pinkerton, L. K. Steinrauf and P. Dawkins, *Biochem. Biophys. Res. Commun.*, 1969, **35**, 512.
13 V. F. Bystrov, Y. D. Gavrilov, V. T. Ivanov and Yu. A. Ovchinnikov, *Eur. J. Biochem.*, 1977, **78**, 63.
14 S. L. Mayo, B. D. Olafson and W. A. Goddard III, *J. Phys. Chem.*, 1990, **94**, 8897.
15 N. Sakurai, K. A. Koike, Y. Irie and H. Hayashi, *Microbiol. Immunol.*, 1994, **38**, 339.
16 M. Bodanszky and A. Bodanszky, *The Practice of Peptide Synthesis*, ed. K. Hafner, Springer-Verlag, Berlin, 1984, vol. 21, pp. 143 and 153.

Paper 4/06937D
Received 14*th November* 1994
Accepted 28*th November* 1994